Catalytic Diversity of Extended Hammerhead Ribozymes[†]

Irina V. Shepotinovskaya and Olke C. Uhlenbeck*

Department of Biochemistry, Molecular Biology, and Cellular Biology, Northwestern University, 2205 Tech Drive, Hogan 2-100, Evanston, Illinois 60208

Received December 27, 2007; Revised Manuscript Received March 21, 2008

ABSTRACT: Chimeras of the well-characterized minimal hammerhead 16 and nine extended hammerheads derived from natural viroids and satellite RNAs were constructed with the goal of assessing whether their very different peripheral tertiary interactions modulate their catalytic properties. For each chimera, three different assays were used to determine the rate of cleavage and the fraction of full-length hammerhead at equilibrium and thereby deduce the elemental cleavage (k_2) and ligation (k_{-2}) rate constants. The nine chimeras were all more active than minimal hammerheads and exhibited a very broad range of catalytic properties, with values of k_2 varying by 750-fold and k_{-2} by 100-fold. At least two of the hammerheads exhibited an altered dependence of k_{obs} on magnesium concentration. Since much less catalytic diversity is observed among minimal hammerheads that lack the tertiary interactions, a possible role for the different tertiary interaction is to modulate the hammerhead cleavage properties in viroids. For example, differing hammerhead cleavage and ligation rates could affect the steady state concentrations of linear, circular, and polymeric genomes in infected cells.

The hammerhead is a small self-cleaving RNA motif that is found embedded in the genomes of plant viroids and virus satellite RNAs, where it is used for genome cleavage and possibly ligation in a rolling circle replication pathway (*1, 2*). The hammerhead has also been found in the transcripts of certain satellite DNAs (*3*) and in the 3′-untranslated regions of a few *Arabidopsis* mRNAs (*4*), but its function in these cases remains unknown. Although the conserved catalytic core of the hammerhead was identified in 1987 (*5*), it was later discovered that all natural hammerheads contain a tertiary interaction between the ends of helices I and II which increases their activity and permits them to function at the low magnesium concentrations present inside cells (*6, 7*). A crystal structure of such an "extended" hammerhead shows that the conformation of the catalytic core is very different from that seen in the structures of "minimal" hammerheads which lack the tertiary interaction (*8*).

Among the 30 available sequences of natural hammerheads (*3, 4, 9*), the nucleotides in the catalytic core are predominantly conserved with only nucleotides 1.1 (U, C, or A), 3 (C or U), and 7 (U, C, A, or G) showing any variation. In addition, a few hammerheads contain an extra nucleotide between core residues 9 and 10.1 (*5, 10, 11*) or 11.1 and 12 (*12, 13*). In contrast to the core, the peripheral elements that make up the tertiary interaction in natural hammerheads are remarkably diverse. They can involve interactions between two hairpins, a hairpin and an internal loop, or two internal loops that are located at different positions in helices 1 and 2 (*6*). There is also considerable variation in both the size and sequence of the tertiary features. For example, among the 20 different hammerhead sequences currently available which contain an interaction between two hairpins, the size of the loops varies from 3 to 38 nucleotides and no two hammerheads share the identical pair of loop sequences (*9*). Not only does this great diversity in tertiary interactions help to explain why their presence was missed for so long, but it also implies that numerous sequences can make a productive tertiary interaction. Indeed, an in vitro selection experiment identified numerous additional tertiary interactions not found in biology which also enhanced the cleavage rate (*14*). Analysis of one of these indicated that it promoted cleavage hundreds of times faster than minimal hammerheads (*15*).

The goal of this paper is to evaluate whether the sequence diversity observed among natural hammerheads results in any difference in their biochemical properties. Although quite different cleavage rates have been reported for several natural hammerheads (*7, 10, 16, 17*), the reaction protocols differed and the buffer conditions often varied significantly. In addition, in most cases, it was not determined whether the extent of cleavage at long incubation reflected the true equilibrium between cleavage and ligation or was reduced by the presence of a fraction of catalytically inactive molecules. If a significant fraction of the hammerheads are misfolded and therefore catalytically inactive, the deduced catalytic rate constants will be incorrectly estimated. This work compares chimeric versions of nine natural hammerheads with differing sequences which all contain hairpins at the ends of helices 1 and 2. Three different assays are used to assess their activities and estimate the fraction of active molecules. We clearly establish that each extended hammerhead has a unique set of catalytic properties.

[†] This work was supported by Grant R01GM36944-22 from the National Institutes of Health and Grant 1C06RR018850-01 from the National Center for Research Resources, a component of the National Institutes of Health.

* To whom correspondence should be addressed. Telephone: (847) 491-5139. Fax: (847) 491-5444. E-mail: uhlenbeck@northwestern.edu.

10.1021/bi7025358 CCC: $40.75
Published on Web 06/11/2008

MATERIALS AND METHODS

RNA Synthesis. The natural hammerhead RNA sequences were selected from the Subviral RNA Database (*9*). All RNAs were in vitro transcribed with T7 RNA polymerase using primer-extended synthetic DNAs as templates (modified from ref *18*). The transcribed and cotranscriptionally cleaved portion of the product was purified on denaturing polyacrylamide gels as described previously (*19*). The uncleaved hammerheads were transcribed in the presence of inhibitory oligonucleotides and [α-^{32}P]ATP at 25 °C as described previously (*6, 7, 19, 20*). During elution of the uncleaved transcript, extensive cleavage was observed even in the presence of 5 mM EDTA.[1] To reduce this high level of self-cleavage, gel elution was performed in 40% formamide and 5 mM EDTA. Purified full-length hammerheads were stored at −20 °C in the presence of 0.2 mM EDTA to prevent cleavage. The 9mer substrate (P1) for the ligation reaction was prepared using the HH16 ribozyme to cleave a 12mer substrate strand (P1-GUC) from Thermo-Fisher (Dharmacon, Boulder, CO) as previously described (*19*). The resulting P1 contained >10% uncleaved 12mer which was unreactive in ligation and therefore could be used without purification. Since hydrolysis of P1 to P1 2′(3′)-phosphate results in a slightly faster moving band on denaturing polyacrylamide gels, the absence of this side reaction was confirmed for all the ligation reactions performed in this study.

Kinetics. Ligation assays were performed under single-turnover conditions with a saturating concentration (1 μM) of ribozyme and a trace concentration (<10 nM) of [5′-^{32}P]P1 as described previously (*19, 21*). Native gels [15% PAG/50 mM Tris-acetate (pH 7.5), 10 mM magnesium acetate; loading buffer, 50% sucrose, 0.02% bromophenol blue, and 0.02% xylene cyanol] were used to confirm that all the P1 formed a complex with Rz. k_{obs}(L) measurements of the very fast nHH3 and nHH8 were performed on a quench flow device (Kintek RQF-3). Rz (1 μM) was annealed to trace (<10 nM) [5′-^{32}P]P1 in either MES (pH 6.0) with 0.4 mM EDTA or 50 mM HEPES (pH 7.3) with 0.4 mM EDTA and was loaded into one sample loop. Either 2 or 20 mM $MgCl_2$ in each buffer was loaded into the second sample loop. Reactions were initiated by delivering equal volumes (~15 μL) of both samples into the reaction loop. Reactions were then quenched at the appropriate time with 86 μL of 7 M urea and 50 mM EDTA. From each time point, 16 μL was analyzed by gel electrophoresis. Intramolecular hammerhead cleavage was performed as described previously (*6, 7, 19, 20*). To determine k_{obs}(C), full-length transcripts were incubated in 50 μL of 50 mM MES (pH 6.0) and 0.2 mM EDTA at 95 °C for 2 min and slowly cooled to 25 °C, and 50 μL of 2.2 mM $MgCl_2$ in 50 mM MES (pH 6.0) was added to start the reactions. Reactions were terminated with 3× stop buffer (1× TBE/7 M urea, 50 mM EDTA, 0.02% bromophenol blue, and xylene cyanol) at different time points and analyzed on 20% PAGE under denaturing conditions. Any RNA that cleaved during purification and preincubation was assumed to cleave during the reaction.

Coupled Transcription Cleavage. The assay was modified from ref *22* and described in detail in ref *19*. A 25 μL transcription mixture contained 2.5 μg of T7 polymerase, NTPs (4 mM each), 10 μCi of [α-^{32}P]ATP, 17 mM $MgCl_2$, and 40 mM Tris-HCl buffer (pH 8.1). Since NTPs and the pyrophosphate product both chelate ions tightly, the final free magnesium concentration remained constant at 1 mM. Reactions were initiated by the addition of 2 μL of 1 μg/μL DNA template. After incubation for 2 h at 25 °C, 5 μL aliquots were quenched with 3× stop buffer and analyzed on 10% polyacrylamide gels.

RESULTS

The RNA secondary structures and genome abbreviations of the nine natural hammerheads chosen for this work are shown in Figure 1. Seven of these natural hammerheads came from either the plus or minus strands of different viroid or satellite viral genomes, while two came from the plus and minus strands of the LTSV genome. The hammerheads were primarily chosen on the basis of having diverse loop 1 and loop 2 sequences; however, extremely large loops were avoided to minimize potential misfolding in the in vitro assays. While the cleavage properties of several (including CChMVd, rCSCVd, PLMVd, and satTRsV) have previously been investigated biochemically (*10, 19, 23, 24*), others (including satSCMoV) have only been shown to cleave in vitro (*25*), while still others (including satCYMoV and satArMV) are proposed only to self-cleave on the basis of their sequence (*11, 26*).

The cleavage and ligation reactions of the nine hammerheads were studied using an approach developed previously for the satTRsV hammerhead (*19*). As shown for one example in Figure 2, the native helix III of each natural hammerhead was replaced with helix III of HH16, a well-characterized minimal hammerhead, to create a chimera. These chimeras were named nHH1−nHH9 (Figure 1), where nHH9 is identical to HH16-T2 derived from satTRsV which we studied previously (*19*). Since the X-ray structure of the extended hammerhead (*8*) shows that helix III does not interact with any other parts of the hammerhead, this substitution is not expected to influence the catalytic properties of the remainder of the molecule. The primary advantage of using chimeras is that the new helix III is sufficiently stable to permit measurement of the reverse ligation reaction while the corresponding helices of several of the natural hammerheads (satLTSV, satArMV, and satTRsV) are too weak to allow stable product binding. An additional experimental convenience is that the same labeled product oligonucleotide, P1, can be used to assay all nine hammerheads. Although helix substitutions can cause long-range effects on the cleavage rates of ribozymes (*27*), there is no indication that this occurs for the hammerhead. Numerous substitutions that modify the sequence and length of helix III of minimal hammerheads have not revealed effects on k_{cat} (*28, 29*). Since it is now clear that the minimal hammerhead goes through the same transition state as extended hammerheads (*30, 31*), it is likely that the cleavage properties of the chimeras will reflect those of the parent molecule.

The catalytic properties of the eight new chimeric hammerheads were initially assayed by measuring the rate and

[1] Abbreviations: HH, hammerhead ribozyme; EPR, electron paramagnetic resonance; Rz, ribozyme; HEPES, *N*-(2-hydroxyethyl)piperazine-*N*′-2-ethanesulfonic acid; PAGE, polyacrylamide gel electrophoresis; MES, 2-(*N*-morpholino)ethanesulfonic acid; FRET, fluorescence resonance energy transfer; NTP, nucleotide triphosphate; EDTA, ethylenediaminetetraacetic acid.

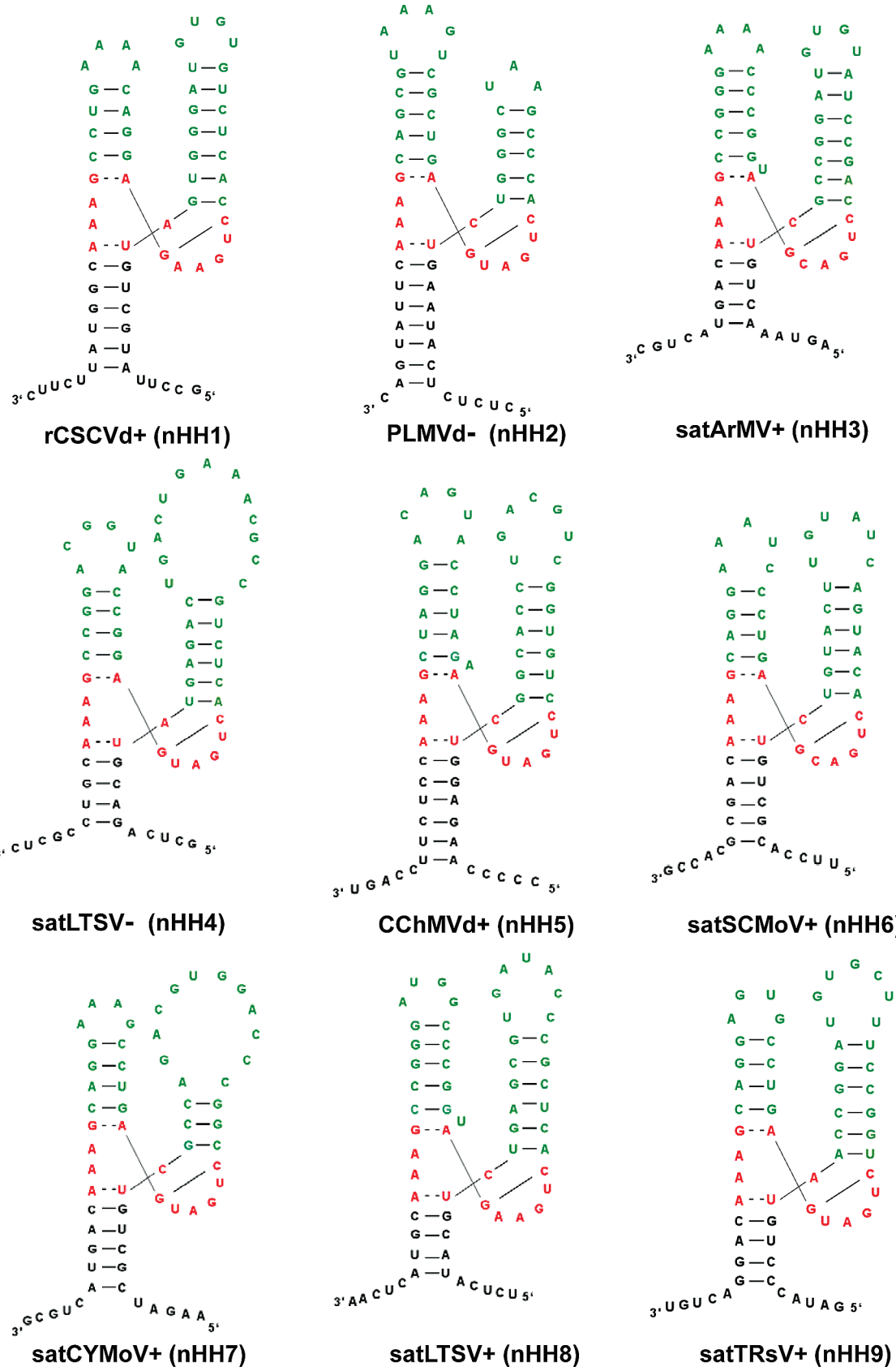

FIGURE 1: Nine hammerheads in native context used to design nHH chimeras. Catalytic cores (red) are arranged to reflect the crystal structure (*8*). Stem III and immediate flanking sequences (black) are replaced in chimeras. Unique hairpins 1 and 2 (green) are also present in chimeras: rCSCVd+ (nHH1), cherry small circular RNA; PLMVd− (nHH2), peach latent mosaic viroid; satArMV+ (nHH3), arabis mosaic virus small satellite RNA; satLTSV− (nHH4) and satLTSV+ (nHH8), lucerne transient streak virus satellite RNA; CChMVd+ (nHH5), chrysanthemum chlorotic mottle viroid; satSCMoV+ (nHH6), subterranean clover mottle satellite RNA; satCYMoVC+ (nHH7), chicory yellow mottle virus satellite RNA; and satTRSV+ (nHH9), satellite of tobacco ringspot virus, where + indicates the genomic strand and − the antigenomic strand.

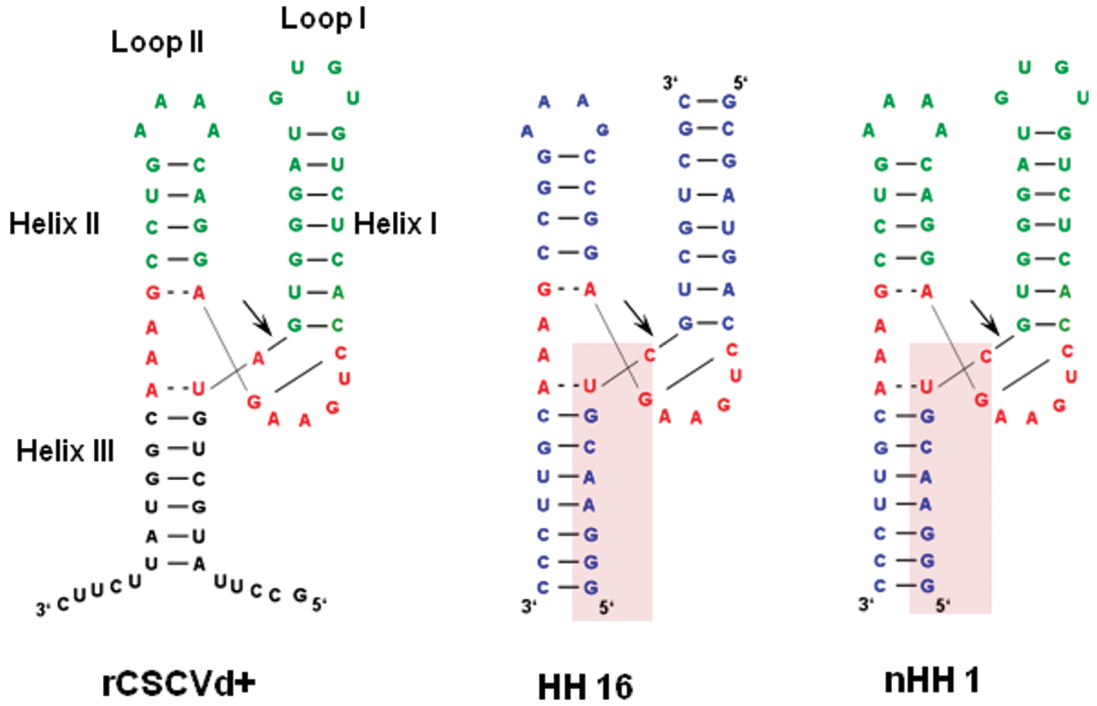

FIGURE 2: Construction of the nHH1 chimera from rCSCVd+ and helix III of HH16 (blue). All chimeras contain the identical nine-nucleotide 5′-cleavage product P1 (highlighted in the pink box on HH16 and nHH1 structures), including a C residue 3′ to the cleavage site (arrow).

extent of the ligation. This was done by annealing a low concentration of 5′-^{32}P-labeled P1 to a saturating concentration of Rz, the remainder of each hammerhead (Figure 3A). As with HH16 (*21*), native gels were used to confirm that >95% of the P1 formed a complex with Rz. Ligation of the Rz·P1 complex was then initiated by the addition of the desired concentration of $MgCl_2$ and the reaction progress followed until equilibrium was reached (Figure 3B). The reaction conditions of 1 mM $MgCl_2$ and 50 mM MES (pH 6.0) at 25 °C were chosen to give reaction rates that in most cases were slow enough that manual pipetting could be used. FRET and EPR experiments have shown that at >0.5 mM $MgCl_2$ the *Schistosoma mansoni* extended hammerhead adopts the helical orientation seen in the crystal structure (*32, 33*). In seven of the nine cases, the data fit well to a single observed rate constant, k_{obs}(L), and a fraction full-length molecule at equilibrium, f_{eq}(L). For nHH3 and nHH8, k_{obs}(L) was too fast to measure manually, but values of f_{eq}(L) could be obtained. The results are summarized in Table 1. The values of k_{obs}(L) varied from 0.024 to >2.5 min^{-1}, and f_{eq}(L) varied from 0.01 to 0.32. While all nine natural hammerheads ligated faster and to a greater extent than the minimal HH16 under the same conditions (k_{obs} = 0.004 min^{-1}; f_{eq} = 0.0075), it is clear that this structurally diverse set of extended chimeric hammerheads have diverse catalytic properties.

To measure k_{obs}(L) for nHH3 and nHH8, a rapid quench flow device was used to add $MgCl_2$ to initiate the reaction and EDTA to terminate the reaction at each desired time point. As summarized in Table 2, nHH3 ligated at 17.3 min^{-1} and nHH8 at 6.8 min^{-1} in the buffer described in Table 1. As reported previously for other extended hammerheads (*15, 16, 34*), the reaction rate increases with both magnesium ion concentration and pH. Under conditions commonly used for minimal hammerheads [10 mM $MgCl_2$ (pH 7.3)], nHH3 exhibits a k_{obs}(L) of 860 min^{-1}, more than 10^3 times faster than the minimal HH16.

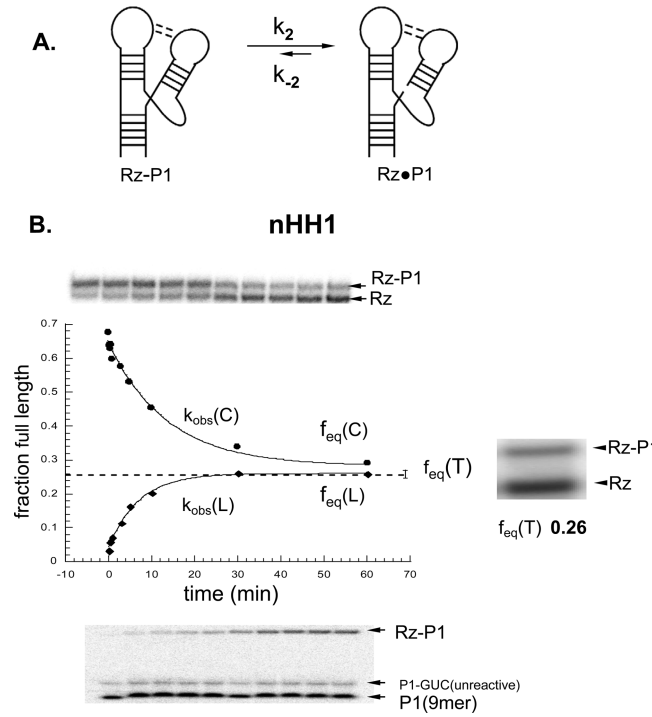

FIGURE 3: Three assays of chimeric hammerheads. (A) Hammerhead cleavage−ligation equilibrium. (B) Example of the approach to equilibrium of nHH1 in cleavage (above) and ligation (below) in 1 mM $MgCl_2$ and 50 mM MES (pH 6.0). Data points show the quantitation of gels, and lines are single-exponential fits to a k_{obs}(C) of 0.074 min^{-1} and an f_{eq}(C) of 0.28 for the cleavage reaction and a k_{obs}(L) of 0.14 min^{-1} and an f_{eq}(L) of 0.26 for the ligation reaction. Example of the coupled transcription cleavage assay (right) performed in 40 mM Tris-HCl (pH 8.1) and 1 mM free $MgCl_2$ at 25 °C gives an f_{eq}(T) of 0.26.

Table 1: Catalytic Properties of Chimeric Hammerheads[a]

	ligation assay		cleavage assay		transcription assay
	k_{obs}(L) (min^{-1})	f_{eq}(L)	k_{obs}(C) (min^{-1})	f_{eq}(C)	f_{eq}(T)
nHH1	0.15 ± 0.05	0.32 ± 0.04	0.08 ± 0.01	0.28 ± 0.009	0.29 ± 0.04
nHH2	1.1 ± 0.28	0.21 ± 0.06	0.89 ± 0.14	0.73 ± 0.03	0.17 ± 0.01
nHH3	>2.5	0.01 ± 0.01	>2.5	0.79 ± 0.04	0.11 ± 0.01
nHH4	0.66 ± 0.04	0.13 ± 0.01	0.59 ± 0.09	0.32 ± 0.03	0.17 ± 0.04
nHH5	2.20 ± 0.18	0.005 ± 0.001	1.2 ± 0.1	0.68 ± 0.05	0.21 ± 0.02
nHH6	1.5 ± 0.06	0.24 ± 0.006	1.2 ± 0.34	0.26 ± 0.05	0.22 ± 0.06
nHH7	0.024 ± 0.01	0.013 ± 0.001	0.077 ± 0.03	0.79 ± 0.08	0.18 ± 0.04
nHH8	>2.5	0.05 ± 0.002	>2.5	0.06 ± 0.004	0.09 ± 0.01
nHH9[b]	0.59 ± 0.10	0.06 ± 0.013	0.54 ± 0.17	0.48 ± 0.08	0.05 ± 0.002

[a] Cleavage and ligation assays were performed in 50 mM MES (pH 6.0) and 1 mM $MgCl_2$ at 25 °C, while transcription assays were conducted in 40 mM Tris-HCl (pH 8.1) and 1 mM free $MgCl_2$ at 25 °C. [b] From ref *19*.

Table 2: k_{obs}(L) Values Measured by Stopped Flow

	k_{obs}(L) (min^{-1})			
	pH 6.0		pH 7.3	
	1 mM $MgCl_2$	10 mM $MgCl_2$	1 mM $MgCl_2$	10 mM $MgCl_2$
nHH3	17 ± 2	30 ± 3	560 ± 60	860 ± 100
nHH8	6.8 ± 1.2	20 ± 4	200 ± 160	470 ± 110

The rates and extents of intramolecular cleavage of the chimeric hammerheads were measured in a second set of assays. Intact, uncleaved hammerheads were prepared by performing in vitro transcription of a complete hammerhead template in the presence of a complimentary DNA oligomer to inhibit cotranscriptional cleavage (*6, 7, 19, 20*). The resulting ^{32}P-labeled uncleaved full-length hammerhead was purified from the inhibitory oligomer on a denaturing gel and then eluted and stored in the absence of divalent ions. After refolding in the reaction buffer, cleavage was initiated by the addition of the desired concentration of $MgCl_2$. As shown for nHH1 in Figure 3B, the time course of the cleavage reaction can be fit to a single observed rate constant, k_{obs}(C), and a fraction of full length at equilibrium, f_{eq}(C). However, analysis of these cleavage experiments was often complicated by the presence of a fraction of cleaved molecules in the starting material that presumably arose from cleavage that occurred during the purification and/or refolding step. This problem was especially acute for hammerheads that cleaved rapidly such as nHH3 and nHH8, so rapid quench experiments were not attempted. The cleavage data for the nine hammerheads are summarized in Table 1. Again, the extended hammerheads are all faster than the minimal HH16 and exhibit substantial differences in their cleavage rates and extents.

The ligation and cleavage assays presumably measure the approach to the same equilibrium between cleaved and uncleaved hammerhead from opposite directions. Thus, the value of k_{obs}(L) should equal k_{obs}(C) since both reflect the sum of the same forward (k_2) and reverse (k_{-2}) elemental rate constants (*29*). Furthermore, if both the cleaved and uncleaved hammerheads are fully active, the two assays should also give the same value of f_{eq}. As shown in Table 1, with the exception of the very fast nHH3 and nHH8 where k_{obs}(C) data are not available, the values of k_{obs}(C) and k_{obs}(L) for each hammerhead indeed agree within a factor of 2, indicating that the two assays are measuring the same reaction. However, f_{eq}(L) and f_{eq}(C) only match well in three of the nine cases tested (nHH1, nHH6, and nHH8). As discussed previously (*19*), this poor agreement of f_{eq} values suggests that a fraction of the hammerhead molecules present in the reaction are inactive in one or both assays. In the case of the cleavage assay, incorporation errors in transcription and incorrect folding during purification can result in a fraction of inactive full-length molecules. This will result in an observed value of f_{eq}(C) that is inappropriately high. In the case of the ligation assay, the starting preparation of Rz must have been active since it was obtained from a self-cleavage reaction. However, a fraction of Rz molecules may not have been folded properly after purification from the denaturing gel, resulting in an abnormally low value of f_{eq}(L). Although different reannealing protocols were tested, the observed disparity between f_{eq}(C) and f_{eq}(L) remained a persistent problem for six of the nine hammerheads.

Since it is important to have a reliable value of f_{eq} to dissect the elemental rate constants, a coupled transcription−cleavage assay was used as an alternative way to obtain f_{eq}. In this assay, each chimeric hammerhead was transcribed from a duplex DNA template using T7 RNA polymerase. The reactions were performed in the 1 nM free $MgCl_2$ concentration used in the other two assays but at a higher pH to permit transcription (*19*). Since the hammerheads fold and cleave during transcription, they are not subjected to the denaturing conditions used for their purification in the other two assays. This minimizes, but may not eliminate, the potential for a fraction of the molecules misfolding into an inactive conformation. While this assay can be used to obtain cleavage rates (*22*), the cleavage rates of the extended hammerheads are too fast compared to the rate of transcription, so only the fraction of full-length molecules at equilibrium, f_{eq}(T), was obtained. As shown in Figure 3B for nHH1, the value of f_{eq}(T) closely matched those of both f_{eq}(L) and f_{eq}(C). This agreement among all three assays strongly suggests that both the cleaved and uncleaved forms of nHH1 are fully active. A similar conclusion can be made for nHH6 and nHH8. In the case of nHH2, nHH4, and nHH9, the f_{eq}(L) and f_{eq}(T) values agree, suggesting that the disparate f_{eq}(C) value is the result of a fraction of inactive full-length molecules present in the cleavage assay. Finally, for three of the hammerheads (nHH3, nHH5, and nHH7), all three f_{eq} values differ and f_{eq}(T) lies between f_{eq}(L) and f_{eq}(C). In these cases, we assume that inactive molecules are present in both the uncleaved and cleaved hammerhead populations and the correct value of f_{eq} is the one obtained in the transcription assay, f_{eq}(T). However, since we cannot exclude the possibility that misfolding also occurs during transcription, the actual value of f_{eq} for these three poorly folding hammerheads must be considered less certain.

Table 3: Calculation of Cleavage and Ligation Rate Constants and K_{int}[a]

	k_{obs} (min^{-1})	f_{eq}	k_2 (min^{-1})	k_{-2} (min^{-1})	K_{int}
nHH1	0.15	0.29	0.11	0.042	2.4
nHH2	1.1	0.17	0.91	0.19	4.9
nHH3	17	0.11	15	1.9	8.1
nHH4	0.66	0.17	0.55	0.11	5.0
nHH5	2.2	0.21	1.7	0.46	3.8
nHH6	1.5	0.22	1.2	0.33	3.5
nHH7	0.024	0.18	0.02	0.004	4.6
nHH8	6.8	0.09	6.2	0.61	10
nHH9[b]	0.59	0.03	0.57	0.018	32
HH16[c]	0.004	0.0075[d]	0.004	3×10^{-5}	130

[a] All values given at 25 °C in 1 mM $MgCl_2$ and 50 mM MES (pH 6.0). Values of k_{obs} and f_{eq} are best estimates based on data in Tables 1 and 2. [b] From ref *19*. [c] From ref *35*. [d] From ref *21*.

The availability of values for k_{obs} and f_{eq} makes it possible to calculate k_2 and k_{-2}, the rate constants for cleavage and ligation, respectively, since $k_{obs} = k_2 + k_{-2}$ and $f_{eq} = k_{-2}/(k_2 + k_{-2})$. As summarized in Table 3, average values of k_{obs} and the best estimate for f_{eq} were used to calculate values for k_2 and k_{-2} for each of the nine hammerheads in 1 mM $MgCl_2$ and 50 mM MES (pH 6.0). All nine chimeric hammerheads exhibit k_2 values that are 5−3750-fold faster than that of the minimal HH16 in the same buffer. Similarly, all the extended hammerheads exhibit values of k_{-2} that are greater than that of HH16 but also vary considerably (475-fold). Interestingly, although the values of k_2 and k_{-2} correlate with one another, the correlation is not perfect. For example, nHH4 and nHH9 have nearly identical k_2 values, and nHH4 has a nearly 5-fold faster k_{-2}. This lack of perfect correlation between k_2 and k_{-2} is also evident in the 13-fold range in the ratio between cleaved and ligated forms at equilibrium that is described by the "internal" equilibrium constants ($K_{int} = k_2/k_{-2}$) in Table 3.

The ligation assay was used to determine k_{obs} as a function of $MgCl_2$ concentration for one of the slowest in the selected hammerheads, nHH1, and two of the faster ones, nHH3 and nHH5. Plots of log(k_{obs}) versus log($MgCl_2$) are presented in Figure 4, along with data reported previously for nHH9 (*19*) and the minimal HH16 (*35*). The slopes of the plots for nHH1 and nHH9 are somewhat less than 1, similar to that of the *S. mansoni* hammerhead (*16*), HH16 (*35*), an in vitro selected extended hammerhead (*15*) and numerous other minimal hammerheads (*36, 37*). However, nHH3 and nHH5 show a nearly second-order dependence of k_{obs} on $MgCl_2$ concentration which has only rarely been observed for hammerheads (*15*). Although many divalent ions bind to the hammerhead, the cleavage rate reports only on the binding of the weakest ion needed to reach the transition state. Although it appears that nHH3 and nHH5 utilize two divalent ions with similar affinities to reach the transition state instead of the usual one, it is unclear whether this reflects an additional divalent ion or whether one of the tighter binding divalent ions binds less well to these hammerheads and thereby also becomes rate-limiting to reach the transition state.

The ligation assay was also used to determine k_{obs} for the extended hammerheads in 2 M LiCl (pH 7.5), HEPES buffer in the absence of divalent ions. As summarized in Table 4, all of the extended hammerheads are not very active in this buffer, showing k_{obs} values only slightly (2−7-fold) faster than that reported for the minimal HH16 under the same conditions. Thus, as previously concluded for nHH9 (*19*) and the *S. mansoni* hammerhead (*16*), it appears that the effect of tertiary interaction is much weaker in LiCl than in buffers containing divalent ions. Either the tertiary interactions do not form in LiCl, or a bound magnesium ion is required for rapid hammerhead cleavage.

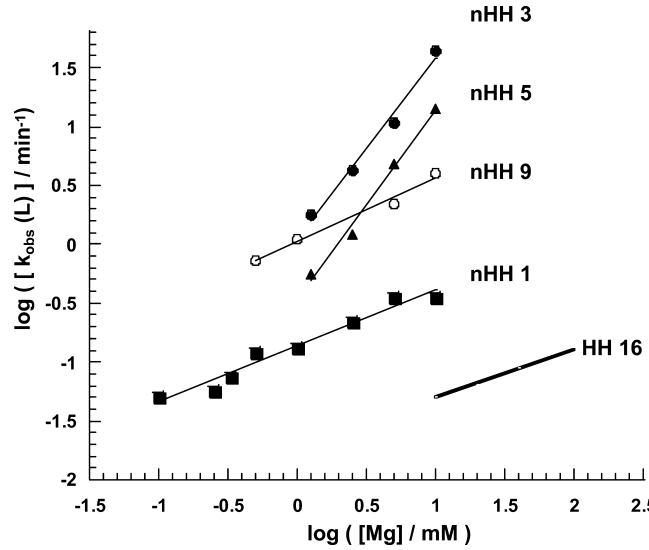

FIGURE 4: Magnesium ion dependence of k_{obs}(L). Although cleavage rates for different hammerheads were determined at different pH values to maximize accuracy, the data were normalized to pH 6.0 using the log-linear pH dependence of cleavage as follows. For nHH1 and nHH9, k_{obs} was determined in 50 mM MES (pH 6.0). For nHH3 and nHH5, k_{obs} values were measured at pH 5.5 and each was multiplied by 3 to correct to pH 6.0. Data for minimal HH16 previously measured at pH 7.5 (*35*) were corrected to pH 6.0 by dividing each rate by 30.

Table 4: k_{obs}(L) Values in 2 M LiCl[a]

hammerhead	k_{obs} (min^{-1})
nHH1	0.12 ± 0.01
nHH2	0.22 ± 0.04
nHH3	0.32 ± 0.1
nHH4	0.12 ± 0.04
nHH5	0.16 ± 0.05
nHH6	0.38 ± 0.08
nHH7	0.0086 ± 0.002
nHH8	0.35 ± 0.02
nHH9	0.16 ± 0.06
HH8[b]	0.05

[a] Rates determined in 50 mM HEPES (pH 7.5) and 2 M LiCl at 25 °C. [b] From ref *18*.

DISCUSSION

The catalytic properties of nine hammerheads containing different peripheral tertiary interactions were compared under uniform reaction conditions. The hammerheads were chosen from more than 20 natural viroid sequences to have tertiary interactions with relatively small hairpin loops to maximize the likelihood that the molecules would fold properly and therefore be active. Although all nine hammerheads exhibited enhanced cleavage and ligation rates compared to hammerheads lacking the tertiary interaction, in six cases the reaction reached a different end point when the equilibrium was approached from opposite directions. This is a clear indication that a significant fraction of the purified full-length hammerhead and/or the cleaved product molecules were not active, either because of errors in transcription or because

they had misfolded or were inactivated during their purification from denaturing gels. The inability to fully renature RNA molecules is well-documented (*38*) and has previously been observed with both extended (*17, 39*) and minimal (*40, 41*) hammerheads. Thus, of the nine extended hammerheads that were tested, only nHH1, nHH6, and nHH8 can be purified in both their cleaved and uncleaved forms as fully active species. These hammerheads are therefore favored candidates for future biochemical and biophysical studies. However, three others (nHH2, nHH4, and nHH9) appear to form fully active cleaved forms and therefore can be studied in ligation reactions.

An estimate of the fraction of full-length molecules at equilibrium permitted the values for the apparent cleavage (k_2) and ligation (k_{-2}) rate constants to be calculated. It is striking that the values of these rate constants are very fast for some of the chimeras. nHH3, the fastest of the nine tested, has a k_2 of 15 min^{-1} in the 1 mM $MgCl_2$ buffer (pH 6.0) used in this study, which increases to >750 min^{-1} in the 10 mM buffer (pH 7.3) more commonly used for measuring hammerhead cleavage rates. Even faster k_2 values would be expected if the pH, $MgCl_2$ concentration, or temperature were increased. k_{obs} values in excess of 800 min^{-1} have also been reported for derivatives of the *S. mansoni* hammerhead (*16*) and the PLMVd hammerhead (*15*) in slightly different buffers. Since k_2 values of 1 min^{-1} are typically observed for minimal hammerheads in 10 mM $MgCl_2$ (pH 7.5) (*21, 29, 41*), this emphasizes the importance of the tertiary interaction for stimulating catalysis. In addition, it is now clear that the "speed limit" for RNA catalysis by the hammerhead mechanism is at least 1000-fold faster than previously thought and even faster cleavage rates may be possible. This may mean that the mechanism is more complex than what was previously thought (*42*).

A second striking feature of the data is that the cleavage and ligation rate constants among the group of nine hammerheads tested are quite diverse. Values of k_2 vary from 0.02 to 15 min^{-1}, and k_{-2} varies from 0.004 to 1.9 min^{-1}. Since the values of k_2 and k_{-2} roughly correlate, this suggests that much of the catalytic diversity is the result of each hammerhead having a slightly different transition state energy. However, since the values of $K_{int} = (k_2/k_{-2})$ vary from 2.4 to 32, this indicates that the relative positions of the cleaved and uncleaved ground states in the reaction free energy diagram are also slightly different. In other words, it appears that the differing hammerhead sequences subtly modify the entire hammerhead reaction profile, leading to their diverse catalytic properties.

Which sequence elements in the extended hammerhead are responsible for the differing catalytic properties? While the catalytic cores of nHH1−nHH9 are not identical, the observed sequence variations at position 7 (U, G, or A) are not expected to significantly modify rates based on experiments with minimal hammerheads (*43*). A residue that is likely to be responsible for some of the catalytic diversity is the "bulged" nucleotide positioned between A9 and G10 (*9*), which substantially enhances cleavage of minimal hammerheads (*10, 44*) and is present in the three fastest hammerheads studied here (nHH3, nHH5, and nHH8). Another source of catalytic diversity could be the varying sequence at the 1.1-1.2 and 2.1-2.2 base pairs which can modify cleavage rates in minimal hammerheads ~10-fold (*45*). Finally, since it is clear that the tertiary interaction dramatically stimulates the catalytic activity, it also may contribute to the diversity in activities. The X-ray structure suggests that the tertiary interaction helps to stabilize the catalytically active core conformation by underwinding helix II and overwinding helix I (*8*). Thus, the structural details of the tertiary interaction as well as the length and sequence of the two helices could potentially affect the structure and/or dynamics of the core and therefore how easily the transition state can be reached. Since the structure and dynamics of the cleaved and uncleaved forms of the hammerhead are likely to be different, each tertiary interaction may affect ground state energies of these forms somewhat differently, leading to different K_{int} values.

An alternate source of catalytic diversity among the different extended hammerheads may be in their differential ability to form the functional tertiary interaction. As originally proposed by Perrachi and Herschlag (*46, 47*), it is now clear that although minimal hammerheads normally adopt a catalytically inactive conformation, they transiently form the same core structure as the extended hammerhead before and after cleavage. Since these conformational isomerizations are very fast compared to the cleavage rate, k_{obs} and f_{eq} can be described by

$$k_{obs} = \left(\frac{K_u}{1+K_u}\right)k'_2 + \left(\frac{1}{1+K_c}\right)k'_{-2}$$

$$f_{eq} = \left(\frac{1}{1+K_c}\right)\frac{k'_{-2}}{k_{obs}}$$

where K_u and K_c are the equilibrium constants describing the conformational change between the inactive and active conformations of the uncleaved and cleaved hammerhead, respectively, and k'_2 and k'_{-2} reflect the "true" elemental rate constants of cleavage and ligation, respectively, and may be the same for all hammerheads (*30*). While K_u and K_c are likely to strongly favor the inactive conformations for minimal hammerheads and strongly favor the active conformation for the very fast extended hammerheads, it is possible that the slower extended hammerheads have intermediate values of K_u and K_c. If this were true, part of the variability of k_{obs} and f_{eq} would be due to the differential ability to form the tertiary interaction. In other words, the slower extended hammerheads may simply have weaker tertiary interactions so that they spend a larger proportion of their time in a conformation that may resemble the catalytically inactive minimal hammerhead structure.

No matter what the underlying structural basis of the catalytic diversity among natural hammerheads turns out to be, it is important to consider why each viroid species has acquired a hammerhead with different sequence and catalytic properties. As with viruses, the small genomes of viroids and satellite RNA are probably highly evolved to fit their individual complex biological niches. Indeed, viroid mutations are often less infectious than their wild-type counterparts and are rapidly lost upon propagation (*48–50*). It therefore seems unlikely that the hammerhead present in a given viroid was simply "frozen" in evolution as one of the many equivalent alternatives, but rather that it was selected to optimize the fitness of the viroid. Hammerheads play a critical role in the replication of viroid genomes by cleaving positive and negative strand genome multimers generated

in their replication pathway (*1*). The resulting linear genome monomers are cyclized in a ligation reaction that in some cases may also be catalyzed by the hammerhead (*51*) and in others by a cellular RNA ligase (*52*). The resulting circles are used as templates for generation of multimers by a rolling circle mechanism (*53, 54*). Analysis of the reaction intermediates by Northern blots indicates that the relative amounts of positive and negative strand multimer, monomer, and circular genomes differ dramatically among different viroids. For example, sASBV-infected cells accumulate primarily positive strand genome multimers and monomer circles (*55*) while PLMVd accumulates roughly equal amounts of positive and negative strand linear monomers and relatively few genome multimers or circles (*54*).

It is possible that the differing catalytic properties of hammerheads present in different viroids could influence the relative steady state concentrations of the reaction intermediates. For example, hammerheads with fast k_{obs} and low f_{eq} values could accumulate linear monomer intermediates, while viroids with hammerheads with slower k_{obs} and greater f_{eq} values could accumulate more multimers or circles. However, there are several reasons why it is inappropriate to directly correlate the data presented here with the Northern blot data. First, since we have measured rates using chimeric hammerheads under nonphysiological conditions, the cleavage and ligation rates of the natural hammerhead sequences in vivo may be considerably different. Second, hammerhead sequences embedded in viral genomes may only transiently fold into an active conformation and then rearrange to an entirely different structure, thereby giving an f_{eq} substantially different than that determined with an isolated hammerhead. Finally, the different forms of viroid genomes could be degraded at different rates, so their relative steady state concentrations may not relate to hammerhead cleavage rates in any simple way. Nevertheless, our observation that different natural hammerheads can have very different intrinsic abilities to cleave and ligate suggests an additional mechanism for how the viroid genome could control its replication pathway.

REFERENCES

1. Symons, R. H. (1997) Plant pathogenic RNAs and RNA catalysis. *Nucleic Acids Res. 25* (14), 2683–2689.
2. Flores, R., Di Serio, F., and Hernandez, C. (1997) Viroids: The non coding genomes. *Semin. Virol. 8*, 65–73.
3. Epstein, L. M., and Gall, J. G. (1987) Self-cleaving transcripts of satellite DNA from the newt. *Cell 48*, 535–543.
4. Przybilski, R., Graf, S., Lescoute, A., Nellen, W., Westhof, E., Steger, G., and Hammann, C. (2005) Functional hammerhead ribozymes naturally encoded in the genome of *Arabidopsis thaliana*. *Plant Cell 17*, 1877–1885.
5. Forster, A. C., and Symons, R. H. (1987) Self-cleavage of plus and minus RNAs of a virusoid and a structural model for the active sites. *Cell 49* (2), 211–220.
6. Khvorova, A., Lescoute, A., Westhof, E., and Jayasena, S. D. (2003) Sequence elements outside the hammerhead ribozyme catalytic core enable intracellular activity. *Nat. Struct. Biol. 10* (9), 708–712.
7. De la Pena, M., Gago, S., and Flores, R. (2003) Peripheral regions of natural hammerhead ribozymes greatly increase their self-cleavage activity. *EMBO J. 22* (20), 5561–5570.
8. Martick, M., and Scott, W. G. (2006) Tertiary contacts distant from the active site prime a ribozyme for catalysis. *Cell 126*, 309–320.
9. Rocheleau, L., and Pelchat, M. (2006) The Subviral RNA Database: A toolbox for viroids, the hepatitis delta virus and satellite RNAs research. *BMC Microbiol. 6*, 24.
10. De la Pena, M., and Flores, R. (2001) An extra nucleotide in the consensus catalytic core of a viroid hammerhead ribozyme: Implications for the design of more efficient ribozymes. *J. Biol. Chem. 276*, 34586–34593.
11. Kaper, J. M., Tousignant, M. E., and Steger, G. (1988) Nucleotide sequence predicts circularity and self-cleavage of 300-ribonucleotide satellite of arabis mosaic virus. *Biochem. Biophys. Res. Commun. 154*, 318–325.
12. Hernandez, C., Daros, J. A., Elena, S. F., Moya, A., and Flores, R. (1992) The strands of both polarities of a small circular RNA from carnation self-cleave in vitro through alternative double- and single-hammerhead structures. *Nucleic Acids Res. 20*, 6323–6329.
13. Song, S. I., Silver, S. L., Aulik, M. A., Rasochova, L., Mohan, B. R., and Miller, W. A. (1999) Satellite cereal yellow dwarf virus-RPV (satRPV) RNA requires a douXble hammerhead for self-cleavage and an alternative structure for replication. *J. Mol. Biol. 293*, 781–793.
14. Saksmerprome, V., Roychowdhury-Saha, M., Jayasena, S., Khvorova, A., and Burke, D. H. (2004) Artificial tertiary motifs stabilize trans-cleaving hammerhead ribozymes under conditions of submillimolar divalent ions and high temperatures. *RNA 10*, 1916–1924.
15. Roychowdhury-Saha, M., and Burke, D. H. (2006) Extraordinary rates of transition metal ion-mediated ribozyme catalysis. *RNA 12*, 1846–1852.
16. Canny, M. D., Jucker, F. M., Kellogg, E., Khvorova, A., Jayasena, S. D., and Pardi, A. (2004) Fast cleavage kinetics of a natural hammerhead ribozyme. *J. Am. Chem. Soc. 126* (35), 10848–10849.
17. Przybilski, R., and Hammann, C. (2007) Idiosyncratic cleavage and ligation activity of individual hammerhead ribozymes and core sequence variants thereof. *J. Biol. Chem. 388*, 737–741.
18. O'Rear, J. L., Wang, S., Feig, A. L., Beigelman, L., Uhlenbeck, O. C., and Herschlag, D. (2001) Comparison of the hammerhead cleavage reactions stimulated by monovalent and divalent cations. *RNA 7*, 537–545.
19. Nelson, J. A., Shepotinovskaya, I., and Uhlenbeck, O. C. (2005) Hammerheads derived from sTRSV show enhanced cleavage and ligation rate constants. *Biochemistry 44*, 14577–14585.
20. Carbonell, A., De la Pena, M., Flores, R., and Gago, S. (2006) Effects of the trinucleotide preceding the self-cleavage site on eggplant latent viroid hammerheads: Differences in co- and post-transcriptional self-cleavage may explain the lack of trinucleotide AUC in most natural hammerheads. *Nucleic Acids Res. 34*, 5613–5622.
21. Hertel, K. J., Herschlag, D., and Uhlenbeck, O. C. (1994) A kinetic and thermodynamic framework for the hammerhead ribozyme reaction. *Biochemistry 33*, 3374–3385.
22. Long, D. M., and Uhlenbeck, O. C. (1994) Kinetic characterization of intramolecular and intermolecular hammerhead RNAs with stem II deletions. *Proc. Natl. Acad. Sci. U.S.A. 91* (15), 6977–6981.
23. Hernandez, C., and Flores, R. (1992) Plus and minus RNAs of peach latent mosaic viroid self-cleave in vitro via hammerhead structures. *Proc. Natl. Acad. Sci. U.S.A. 89*, 3711–3715.
24. Di Serio, F., Daros, J. A., Ragozzino, A., and Flores, R. (1997) A 451-nucleotide circular RNA from cherry with hammerhead ribozymes in its strands of both polarities. *J. Virol. 71*, 6603–6610.
25. Davies, C., Haseloff, J., and Symons, R. H. (1990) Structure, self-cleavage, and replication of two viroid-like satellite RNAs (virusoids) of subterranean clover mottle virus. *Virology 177*, 216–224.
26. Rubino, L., Tousignant, M. E., Steger, G., and Kaper, J. M. (1990) Nucleotide sequence and structural analysis of two satellite RNAs associated with chicory yellow mottle virus. *J. Gen. Virol. 71* (Part 9), 1897–1903.
27. Tinsley, R. A., and Walter, N. G. (2007) Long-range impact of peripheral joining elements on structure and function of the hepatitis delta virus ribozyme. *Biol. Chem. 388*, 705–715.
28. Fedor, M. J., and Uhlenbeck, O. C. (1990) Substrate sequence effects on "hammerhead" RNA catalytic efficiency. *Proc. Natl. Acad. Sci. U.S.A. 87*, 1668–1672.
29. Stage-Zimmermann, T. K., and Uhlenbeck, O. C. (1998) Hammerhead ribozyme kinetics. *RNA 4* (8), 875–889.
30. Nelson, J. A., and Uhlenbeck, O. C. (2008) Minimal and extended hammerheads utilize a similar dynamic reaction mechanism for catalysis. *RNA 14*, 43–54.
31. Nelson, J. A., and Uhlenbeck, O. C. (2008) Hammerhead Redux: Does the new structure fit the old biochemical data? *RNA* (in press).

32. Penedo, J. C., Wilson, T. J., Jayasena, S. D., Khvorova, A., and Lilley, D. M. (2004) Folding of the natural hammerhead ribozyme is enhanced by interaction of auxiliary elements. *RNA 10*, 880–888.
33. Kim, N. K., Murali, A., and DeRose, V. J. (2005) Separate metal requirements for loop interactions and catalysis in the extended hammerhead ribozyme. *J. Am. Chem. Soc. 127*, 14134–14135.
34. Osborne, E. M., Schaak, J. E., and Derose, V. J. (2005) Characterization of a native hammerhead ribozyme derived from schistosomes. *RNA 11*, 187–196.
35. Clouet-d'Orval, B., Stage, T. K., and Uhlenbeck, O. C. (1995) Neomycin inhibition of the hammerhead ribozyme involves ionic interactions. *Biochemistry 34* (35), 11186–11190.
36. Inoue, A., Takagi, Y., and Taira, K. (2004) Importance in catalysis of a magnesium ion with very low affinity for a hammerhead ribozyme. *Nucleic Acids Res. 32*, 4217–4223.
37. Rueda, D., Wick, K., McDowell, S. E., and Walter, N. G. (2003) Diffusely bound Mg^{2+} ions slightly reorient stems I and II of the hammerhead ribozyme to increase the probability of formation of the catalytic core. *Biochemistry 42*, 9924–9936.
38. Uhlenbeck, O. C. (1995) Keeping RNA happy. *RNA 1* (1), 4–6.
39. Canny, M. D., Jucker, F. M., and Pardi, A. (2007) Efficient ligation of the *Schistosoma* hammerhead ribozyme. *Biochemistry 46*, 3826–3834.
40. Clouet-D'Orval, B., and Uhlenbeck, O. C. (1996) Kinetic characterization of two I/II format hammerhead ribozymes. *RNA 2* (5), 483–491.
41. Fedor, M. J., and Uhlenbeck, O. C. (1992) Kinetics of intermolecular cleavage by hammerhead ribozymes. *Biochemistry 31* (48), 12042–12054.
42. Emilsson, G. M., Nakamura, S., Roth, A., and Breaker, R. R. (2003) Ribozyme speed limits. *RNA 9*, 907–918.
43. Ruffner, D. E., Stormo, G. D., and Uhlenbeck, O. C. (1990) Sequence requirements of the hammerhead RNA self-cleavage reaction. *Biochemistry 29* (47), 10695–10702.
44. Warashina, M., Kuwabara, T., Nakamatsu, Y., Takagi, Y., Kato, Y., and Taira, K. (2004) Analysis of the conserved P9-G10.1 metal-binding motif in hammerhead ribozymes with an extra nucleotide inserted between A9 and G10.1 residues. *J. Am. Chem. Soc. 126*, 12291–12297.
45. Clouet-d'Orval, B., and Uhlenbeck, O. C. (1997) Hammerhead ribozymes with a faster cleavage rate. *Biochemistry 36* (30), 9087–9092.
46. Peracchi, A., Beigelman, L., Usman, N., and Herschlag, D. (1996) Rescue of abasic hammerhead ribozymes by exogenous addition of specific bases. *Proc. Natl. Acad. Sci. U.S.A. 93*, 11522–11527.
47. Peracchi, A., Karpeisky, A., Maloney, L., Beigelman, L., and Herschlag, D. (1998) A core folding model for catalysis by the hammerhead ribozyme accounts for its extraordinary sensitivity to abasic mutations. *Biochemistry 37*, 14765–14775.
48. Gago, S., De la Pena, M., and Flores, R. (2005) A kissing-loop interaction in a hammerhead viroid RNA critical for its in vitro folding and in vivo viability. *RNA 11*, 1073–1083.
49. Owens, R. A., Thompson, S. M., and Steger, G. (1991) Effects of random mutagenesis upon potato spindle tuber viroid replication and symptom expression. *Virology 185*, 18–31.
50. Niblett, C. L., Dickson, E., Fernow, K. H., Horst, R. K., and Zaitlin, M. (1978) Cross protection among four viroids. *Virology 91*, 198–203.
51. Flores, R., Daros, J. A., and Hernandez, C. (2000) Avsunviroidae family: Viroids containing hammerhead ribozymes. *Adv. Virus Res. 55*, 271–323.
52. Gas, M. E., Hernandez, C., Flores, R., and Daros, J. A. (2007) Processing of nuclear viroids in vivo: An interplay between RNA conformations. *PLoS Pathog. 3*, e182.
53. Branch, A. D., and Robertson, H. D. (1984) A replication cycle for viroids and other small infectious RNA's. *Science 223*, 450–455.
54. Bussiere, F., Lehoux, J., Thompson, D. A., Skrzeczkowski, L. J., and Perreault, J. (1999) Subcellular localization and rolling circle replication of peach latent mosaic viroid: Hallmarks of group A viroids. *J. Virol. 73*, 6353–6360.
55. Daros, J. A., Marcos, J. F., Hernandez, C., and Flores, R. (1994) Replication of avocado sunblotch viroid: Evidence for a symmetric pathway with two rolling circles and hammerhead ribozyme processing. *Proc. Natl. Acad. Sci. U.S.A. 91*, 12813–12817.

BI7025358